


Please cite the Published Version

Biswas, Sayan, Sarkar, Ved, MacArthur, Joshua Ian, Guo, Li , Deng, Xutao, Snowdon, Ella, Ahmed, Hamza, Tetlow, Callum and George, K Joshi (2025) Development of a machine learning algorithm to identify cauda equina compression on MRI scans. *World Neurosurgery*, 195. 123669 ISSN 1878-8750

DOI: <https://doi.org/10.1016/j.wneu.2025.123669>

Publisher: Elsevier

Version: Published Version

Downloaded from: <https://e-space.mmu.ac.uk/638280/>

Usage rights:  [Creative Commons: Attribution 4.0](https://creativecommons.org/licenses/by/4.0/)

Additional Information: This is an open access article which first appeared in *World Neurosurgery*

Enquiries:

If you have questions about this document, contact openresearch@mmu.ac.uk. Please include the URL of the record in e-space. If you believe that your, or a third party's rights have been compromised through this document please see our Take Down policy (available from <https://www.mmu.ac.uk/library/using-the-library/policies-and-guidelines>)



Development of a Machine-Learning Algorithm to Identify Cauda Equina Compression on Magnetic Resonance Imaging Scans

Sayan Biswas¹, Ved Sarkar², Joshua Ian MacArthur³, Li Guo⁴, Xutao Deng⁵, Ella Snowden¹, Hamza Ahmed⁶, Callum Tetlow⁷, K. Joshi George⁸

■ **OBJECTIVE:** Cauda equina syndrome (CES) poses significant neurological risks if untreated. Diagnosis relies on clinical and radiological features. As the symptoms are often nonspecific and common, the diagnosis is usually made after a magnetic resonance imaging (MRI) scan. A huge number of MRI scans are done to exclude CES but nearly 80% of them will not have CES. This study aimed to develop and validate a machine-learning model for automated CES detection from MRI scans to enable faster triage of patients presenting with CES like clinical features.

■ **METHODS:** MRI scans from suspected CES patients (2017–2022) were collected and categorized into normal scans/disc protrusion (0%–50% canal stenosis) and cauda equina compression (>50% canal stenosis). A convolutional neural network was developed and tested on a total of 715 images (80:20 split). Gradient descent heatmaps were generated to highlight regions crucial for classification.

■ **RESULTS:** The model achieved an accuracy of 0.950 (0.921–0.971), a sensitivity of 0.969 (0.941–0.987), a specificity of 0.859 (0.742–0.937), a positive predictive value of 0.969 (0.944–0.984), and an area under the curve of 0.915 (0.865–0.958). Gradient descent heatmaps demonstrated

accurate identification of any clinically relevant disc herniation into the spinal canal.

■ **CONCLUSIONS:** This study pilots a deep learning approach for predicting cauda equina compression presence, promising improved healthcare quality and timely CES management. As referrals rise, this tool can act as a fast triage system which can lead to prompt management of CES in environments where resources for radiological interpretation of MRI scans are limited.

INTRODUCTION

Cauda equina syndrome (CES) is a rare but potentially devastating condition that, when left untreated, can result in permanent paralysis, bowel and bladder dysfunction, loss of sexual sensation, and chronic pain. CES is most commonly caused by intervertebral disc herniation resulting in compression of the nerve roots of the cauda equina. In the United Kingdom, the incidence of the condition is estimated between 0.3 and 1.9 cases per 100,000 persons.^{1,2}

Key words

- Cauda equina compression
- CNN
- Mid-sagittal MRI

Abbreviations and Acronyms

CEC: Cauda equina compression

CES: Cauda equina syndrome

DP: Disc prolapse

GIRFT: Get It Right First Time

Grad-CAM: Gradient-weighted Class Activation Mapping

ML: Machine-learning

MRI: Magnetic resonance imaging

NHS: National Health Service

PCR: Prolapse to canal ratio

VGG: Visual Geometry Group

Berkeley, California, USA; ³Department of Surgery and Cancer, Imperial College London, Northwick Park Hospital, London Northwest University Healthcare, Harrow, England, United Kingdom; ⁴Department of Computer Science, Manchester Metropolitan University, Manchester, England, United Kingdom; ⁵Department of Electrical Engineering, Edge Hill University, Lancashire, England, United Kingdom; ⁶Department of Trauma and Orthopaedics, Salford Royal Hospital, Manchester, England, United Kingdom; ⁷Department of Data Science, Northern Care Alliance, Manchester, England, United Kingdom; and ⁸Department of Neurosurgery, Manchester Centre for Clinical Neurosciences, Salford Royal Hospital, Manchester, England, United Kingdom

To whom correspondence should be addressed: Sayan Biswas, M.B.Ch.B., M.Res.
[E-mail: sayan.biswas@nca.nhs.uk]

Citation: *World Neurosurg.* (2025) 195:123669.

<https://doi.org/10.1016/j.wneu.2025.123669>

Journal homepage: www.journals.elsevier.com/world-neurosurgery

Available online: www.sciencedirect.com

1878-8750/© 2025 The Authors. Published by Elsevier Inc. This is an open access article under the CC BY license (<http://creativecommons.org/licenses/by/4.0/>).

From the ¹Specialized Foundation Doctor Training Programme, Edge Hill University, Omskirk, England, United Kingdom; ²College of Letters and Sciences, University of California,

CES does not have a definitive clinical definition and presenting symptomatology. Clinical features of CES do not always correlate to radiological findings on magnetic resonance imaging (MRI), with less than 20% of these cases having radiological features suggestive of CES. True CES is defined as the presence of cauda equina compression (CEC) on radiology with associated clinical signs and symptoms of CES.^{2,3} Current UK guidelines recommend urgent referral for emergency assessment with MRI for any case of suspected CES presenting within 2 weeks of symptom onset. This results in ~8000 scans for suspected CES each year, placing a huge burden on tertiary spinal units which are already overburdened with referrals.⁴ Moreover, the Receipt Royal Society Report estimates a shortage of ~2000 radiologists across the United Kingdom.⁵ The huge number of scans done nationwide every day for suspected CES cases coupled with the shortage of radiologists nationally leads to further delays in the diagnosis of this time critical condition.

From a litigation perspective, delay in the provision of care for CES is associated with huge medicolegal costs in addition to disease morbidity. Machin et al. identified CES as the most common cause of litigation for acute spinal presentations and damage pay-outs.⁶ Delays in the definitive diagnosis and subsequent surgical treatment result in patients suffering with long-term morbidity with disabling sphincter and lower limb deficits as well as severe pain. It has been estimated that litigation from improper management of CES costs the National Health Service (NHS) 68 million pounds per year.⁷ The NHS Litigation Authority report average damage pay-outs of £211,758 per case.⁸ The Healthcare Safety Investigation Branch's investigation on the timely detection and treatment of CES concluded that there exist major flaws in the provision of care and so there is an imminent national need for clinical decision-making tools to enhance and improve the CES patient pathway.⁹

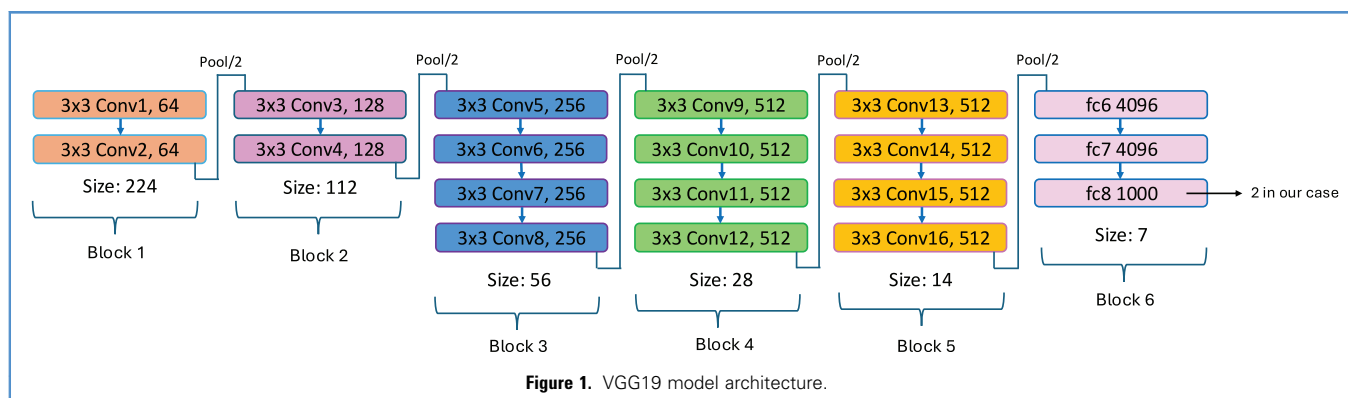
The automated detection of potential CEC from MRI scans using a computer vision model may help to delay identification of CES, improve time to treatment, and decrease morbidity, with recent studies confirming the utility of such techniques in the field of spine surgery.^{10,11} Thus, the aim of this project was to develop and validate a computer vision model that uses MRI sequences to facilitate rapid yet reliable CEC detection, for triaging suspected CES scans.

METHODS

Data Source

This project was a single-center retrospective computer vision analysis of all CES patients at a tertiary neurosurgical center in Manchester from 2017–2022. The trust's database was examined and all patients who had undergone emergency lumbar discectomy over this time period were extracted. The International Classification of Diseases, 10th Revision code for CES is G38.4. This code was then used to filter out the CES patients from the total cohort. The hospital's online picture archiving and communication system (Sectra UniView) was then queried to blind-download, anonymize, and store the corresponding mid-sagittal T2 MRI scans for these patients. Following the Get It Right First Time (GIRFT) guidance in the United Kingdom, only mid-sagittal scans were used for developing the model.¹² Patients with chronic canal stenosis were not included in this study as per the GIRFT guidance and neither were patients who had difficult to visualize levels (e.g., those who had metalwork in the spine). Next, the remaining patients from the total cohort were analyzed to determine the number of patients with an underlying diagnosis of lumbar disc prolapse (DP) and their corresponding scans were respectively downloaded. Finally, a cohort of normal MRI lumbar spine scans was collected from patients with no lumbar spine pathology under the senior author's care. Patient consent was not required as the study was conducted in an anonymized and retrospective manner. The study was approved as a health improvement project by the North West Research and Innovation board, reference number: 22HIP32. NHS Health Research Authority review and approval was deemed unnecessary for this project. All subsequent methods were performed in accordance with the relevant local guidelines and regulations.

These scans were then analyzed and a binary outcome variable of CEC and non-CEC was created. The scans were binarized at a prolapse to canal ratio (PCR) of 50%, with all CEC scans having a PCR of more than 50%, to maximize sensitivity and reduce false negatives. The less than 50% PCR class included both normal and DP scans. The goal was to create a model able to differentiate the key differences between a CEC scan and a non-CEC scan. The presence of CEC, DP, and normal scans were all confirmed by a



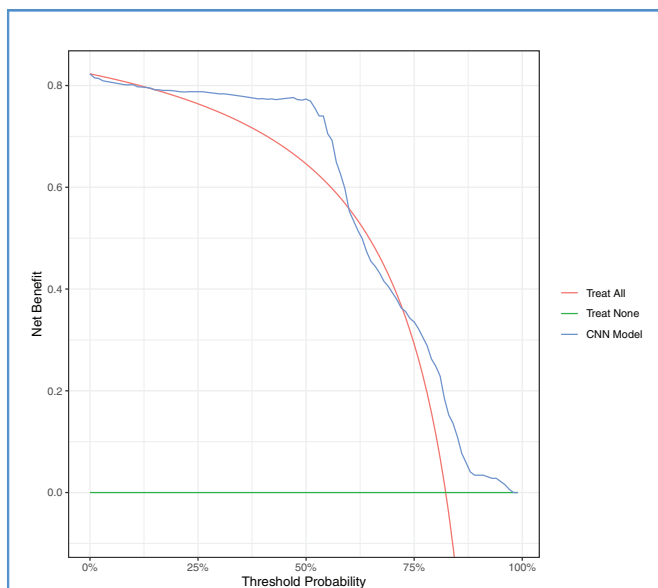


Figure 2. Decision curve analysis comparing the model's decision-making to that of the default strategies.

senior consultant neurosurgeon and the associated radiology reports.

Deep Learning Algorithm: Model Architecture

For this study, we employed the Visual Geometry Group (VGG) 19 convolutional neural network architecture¹³ due to its robustness and proven efficacy in image classification tasks. It is a deep neural network consisting of 19 layers, including 16 convolutional layers and 3 fully connected layers (Figure 1).

The network's design emphasizes simplicity and depth, which are crucial for extracting intricate features from medical images. In addition to VGG19, we experimented with other deep learning architectures, including ResNet,¹⁴ DenseNet,¹⁵ and Vision Transformers.¹⁶ While these architectures are known for their high performance in various image classification tasks, VGG19 demonstrated superior performance in our specific application of detecting CEC in MRI scans. We believe this was attributed to the simplicity and depth of VGG19, which effectively captured the relevant features in the medical images.

Model Training

The training of the network underwent a 2-phase training process, crucial due to the rarity of CEC cases, which challenges traditional supervised learning methods due to limited labeled examples. Initially, the VGG19, pretrained on a large dataset for generic objects,¹⁷ was further fine-tuned using a self-supervised learning method. This first phase involved a public lumbar spine MRI dataset,¹⁸ which includes MRI studies of 515 patients with symptomatic back pain, only 11 of whom were diagnosed with CEC. This approach allowed the model to learn detailed spinal features without relying on extensive labeled MRI data, thus optimizing its ability to identify subtle patterns associated with

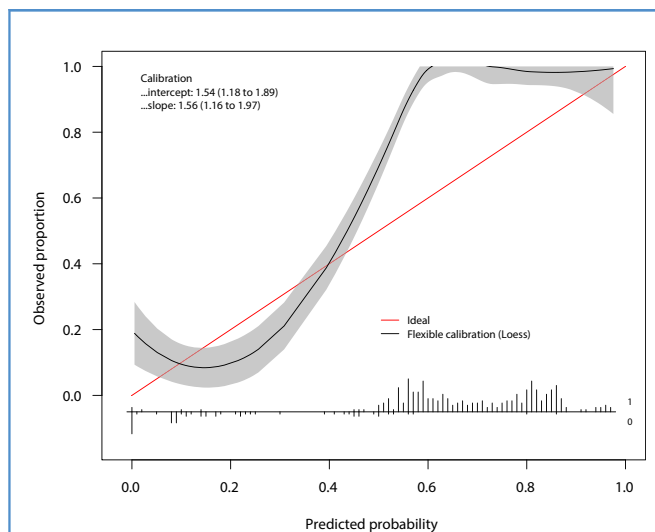
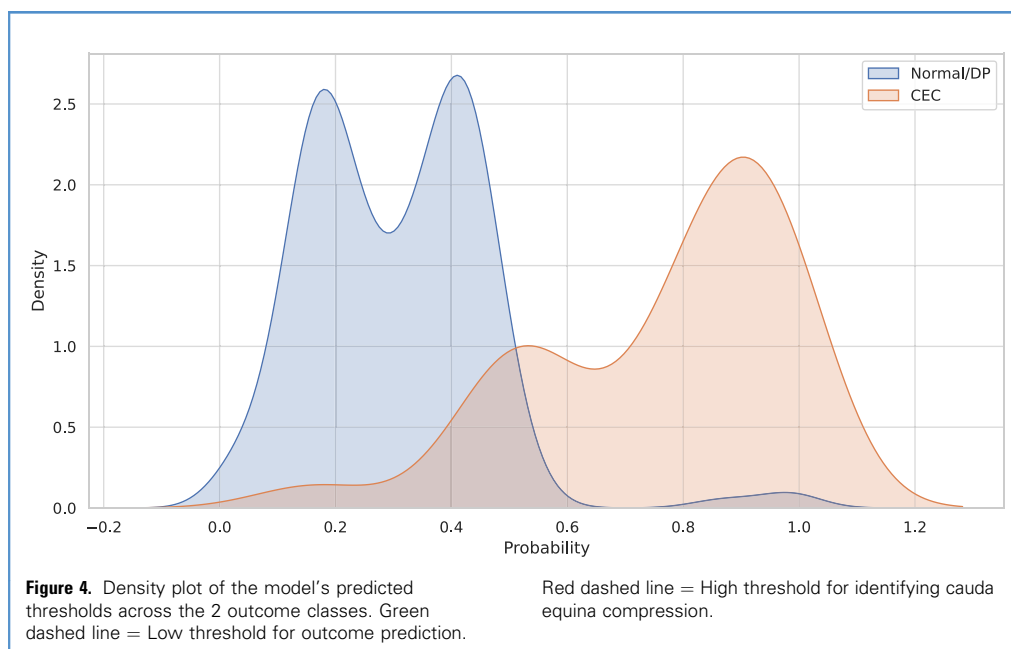


Figure 3. Calibration curve of the model demonstrating the model's approach toward overpredicting the presence of cauda equina compression.

CEC. Self-supervised learning, as described by He et al.,¹⁹ leverages unlabeled data, making it a powerful tool in scenarios where annotated examples are scarce. To use the public dataset and for the ease of processing and compatibility with the VGG19 model, we converted the dataset from the DICOM format to PNG format. This conversion focused on the mid-sagittal view images, crucial for analyzing the lumbar spine and detecting CEC. We further fine-tuned the model using the dataset collected from the Northern Care Alliance. This dataset, comprising mid-sagittal T2 MRI scans from patients at a tertiary neurosurgical center, provided a more focused and relevant set of images. It contains 100 CEC cases and 100 disc-protrusion cases. These 200 cases were combined with the 515 cases from the public dataset and formed our final dataset ($N = 715$). The final dataset was then split with an 80%–20% training-testing split for the final tuning process. The fine-tuning process involved retraining the last few layers of the model on this specialized dataset while keeping the earlier layers frozen to retain the pretrained weights for feature extraction. The final network outputs a 2-class classification.

Model Explainability

To enhance the model's interpretability, Gradient-weighted Class Activation Mapping (Grad-CAM)²⁰ was used, which provides visual explanations for the decisions made by the trained network. Grad-CAM uses the gradients of any target concept flowing into the final convolutional layer to produce a coarse localization map highlighting the important regions in the image for predicting the concept. This technique was particularly useful in our study to verify that the model's predictions were based on the correct anatomical features of the spine relevant to CEC and disc protrusion. It not only helped in validating the model's diagnostic reasoning but also in building trust with clinicians by



showing that the model focuses on plausible areas when diagnosing conditions. This visualization is essential for clinical presentations and further development of the model, ensuring that its decisions can be audited for accuracy and reliability.

Statistical Analysis

For each fold, the model's performance was evaluated via analysis of the accuracy, positive predictive value, negative predictive value, specificity, sensitivity, area under the receiver operating curve/discrimination, and the brier score loss. All metrics were bootstrapped to derive the associated 95% confidence intervals. Each model was then calibrated on the testing set. Additionally, decision curve analysis was used to evaluate and plot the clinical benefit of using the computer vision algorithms to predict the presence of CEC over a wide range of predicted threshold probabilities. This illustrates the net benefit defined as the number of true positives detected for each outcome class when using the computer vision algorithm.

RESULTS

The average age of the cohort was 50.10 ± 15.11 years and 53.65% of patients were female. Detailed cohort demographic data were not collected for this study with a focus on the collection and anonymization of the lumbar MRI scans, and model development.

Model Performance

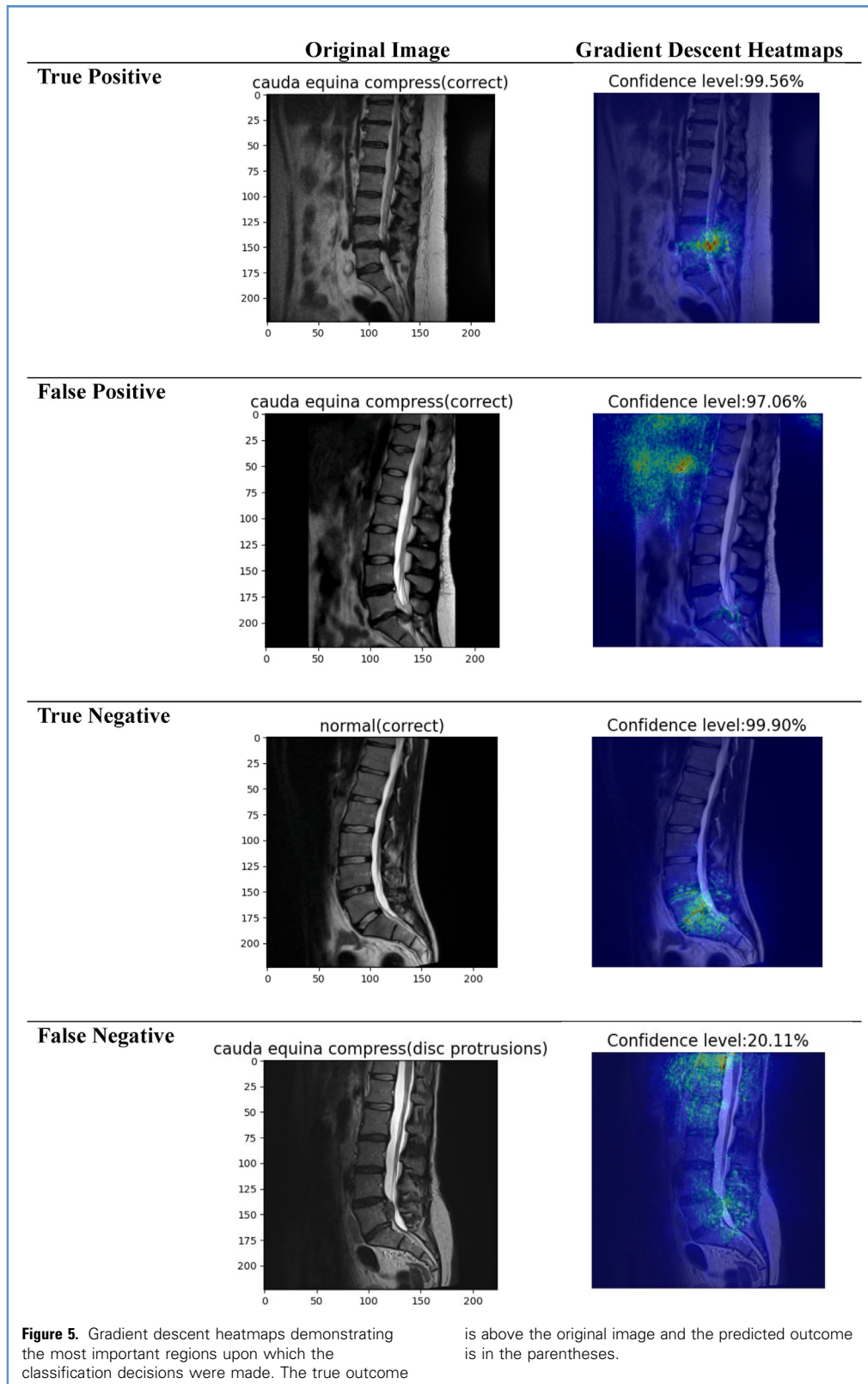
The optimally trained model was evaluated on the test set. On the holdout set, the model achieved an accuracy of 0.950 (0.921–0.971), a sensitivity of 0.969 (0.941–0.987), a specificity of 0.859 (0.742–0.937), a positive predictive value of 0.969 (0.944–0.984), a negative predictive value of 0.856 (0.754–0.924), and an area under the curve of 0.915 (0.865–0.958). Decision curve analysis

demonstrated that the machine-learning (ML) model provided greater clinical net benefit in correctly identifying radiological CEC at all predicted probabilities relative to the default strategies of identifying of all or no patients, except between the threshold probability of 55% and 72%. This demonstrates that the model's predictions for scans falling within that threshold range may not be better than the default strategies (Figure 2).

Model Decision-Making

The calibration curve of this model demonstrates the model's liberal approach of predicting the presence of CEC after a 40% threshold is reached (Figure 3). The curve has an intercept of 1.54 (1.18–1.89), a slope of 1.56 (1.16–1.97), and the model has a Brier score loss of 0.049 (0.027–0.075). Density plot of the model's decision-making further highlights that the 2 output categories have significant overlap in terms of the thresholds for predicting either outcome class. There is a significant overlap between the 2 classes within the 0.4–0.65 range. This demonstrates that a higher threshold of suspicion could be used to identify only CEC as demonstrated by the red dashed line in Figure 4. However, there might be a chance of missing CEC when using these thresholds due to lower threshold cases being present, but this may cause normal or DP patients to be misclassified as CEC or vice versa.

This tradeoff is evident by the model's high sensitivity compared to its specificity. The model has a propensity to predict a patient as having CEC from low probability values, thereby increasing false positive rates compared to false negative rates. This probability threshold can be adjusted by changing the threshold used during model training, which in this study was 50% canal stenosis.



Gradient Descent Heatmaps

Grad-CAM heatmaps demonstrate accurate identification of the clinically relevant disc(s) and any associated herniation into the spinal canal (Figure 5). The model is able to look for any disc herniation particularly at the lumbar spine region when differentiating between true positives and true negatives. However, the false positive and false negative heatmaps demonstrate that the model is not only attentive to those regions but also has a propensity to analyze nonsignificant and potentially irrelevant areas for identifying CEC: 1) distant regions of the spine such as the thoracic spine for the false negative scan and 2) the abdominal viscera and vasculature anterior to the spinal column for false positive scan.

DISCUSSION

To our knowledge, this is the first ever study that has performed reliable and automated radiological CEC detection via a computer vision algorithm. Given the large burden of scans done for patients with suspected CES and the low number of scan positive CEC, automated systems that could rapidly triage such scans from most urgent to least and can take place in real time, make this topic area an ideal candidate for ML modeling. This tool would result in a shorter time to reporting by our radiologists and an overall shorter time to surgery for the necessary patients. Thus, in line with the GIRFT guidance that a sagittal T2 sequence is all that is required to screen for and detect CEC, our model has the ability to alert physicians about patients who may need urgent scan reporting and subsequent surgical intervention. A prompt analysis of the mid-sagittal section if flagged as CEC could enable the patient continuing on to a full MRI scan. Similar use of automated detection tools is already being used in clinical practice for triage in other time-critical pathology like stroke, thereby showing the usefulness of such tools in clinical practice.

Our model was successfully able to predict the presence of CEC with good accuracy and visualize the clinically relevant areas to make said prediction. Our model's ability to perform fast yet reliable triage for CES patients is further underscored by the fact that delayed-intervention groups have been shown to have significantly increased rates of inpatient mortality, total complications and nonroutine discharge, compared to prompt intervention groups.²¹ In support of this, our model was able to learn the key differences between normal and non-normal scans and even develop a propensity to overpredict the presence of CEC, to minimize the risk of false negatives.

CES is a complex clinical syndrome resulting in a variety of neurological signs and symptoms. Clinically, patients may report saddle sensory changes, bladder, bowel, or sexual dysfunction, bilateral radicular pain, back pain, lower limb pain, and lower limb neurological deficits. The presence of these red flag symptoms raise suspicion of suspected CES and these patients are thus immediately referred to tertiary neurosurgery spine centers for prompt investigation and management. Radiological confirmation of the etiology of these symptoms is required in each of these patients, with only the presence of both radiological CEC and the aforementioned clinical symptoms confirming the diagnosis of CES.²²

Previous evidence investigating the correlation among history, physical examination, and MRI scan result has interestingly established that the mean prevalence of patients having both clinical and radiological evidence of CES is 14%–48% with no single individual sign or symptom being helpful in diagnosing CES.^{2,12} Additionally, only 13% to 22% of patients with suspected CES symptoms have scan-positive CEC.^{12,22} Balasubramaniam et al. further this sentiment by reporting that even an appropriately trained clinician cannot reliably predict which patient has a CES.²³

This lack of a definite clinical-radiological correlation results in a number of borderline cases such as patients with acute CES like clinical features but no CEC on MRI, that is, scan-negative CES like presentation and those patients with radiological CEC but no clinical symptoms.

In clinical practice, this complex interplay between clinical and radiological findings results in a large number of scans being performed and unsurprisingly being reported as normal, non-CEC scans. Each of these scans has to be meticulously interpreted and reported by a consultant neuroradiologist, causing a back log and delay in the reporting of the most urgent scans. Over the years, the number of MRI scans done for patients with suspected CES has been rapidly increasing, not only due to the uncertainty of a true clinical diagnosis of CES but also due to the clinical and medicolegal repercussions of missing CES.⁴ Thus, an automated triage tool for prioritizing scans to be subsequently reported and verified by a neuroradiologist will greatly benefit our CES patients and improve our quality of care provision.

The PCR is the ratio of the largest width of the disc herniation at the affected spinal level by the total of width of the spinal canal at the level of the herniation. Previous research has stipulated that a herniated disc compressing 75% or more of the spinal canal with associated compression of the cauda equina nerves is CEC. This definition was coined by McCarthy et al. in a study from 2005 measuring the mean PCR in only 12 patients.²⁴

Since then, studies have reported that only a minority of patients fall in this category. Qureshi and Sell found that only 45% of their 33 patients operated for CES and had DPs of this size, while a case series by Kaiser et al. on 55 CES patients observed a mean PCR of 0.6, with a PCR of ≤ 0.5 in 20 patients (38.5%) and ≥ 0.75 in only 12 patients (23%).²⁵ Similarly, our analysis has demonstrated a large distribution of PCR causing CEC despite our lower predefined cutoff of 50%. As a result, there is a lack of interstudy agreement in terms of what counts as a PCR cutoff for a herniated disc capable of causing CES. Furthermore, these aforementioned studies have all reported no significant correlation between radiological PCR and postsurgical clinical outcome. Additionally, studies have demonstrated a poor correlation between PCR and the evolution and severity of neurological deficits.²⁵

As such, these results question the underlying pathophysiological mechanisms of CES, especially as a consequence of lumbar DPs of varying PCR. The traditional view of disc-mediated pressure causing compression of the cauda equina nerve roots is unable to explain the varied radiological findings in this patient cohort. Alternative supplementary hypotheses including differences in microvascular spinal anatomy, postherniation inflammatory responses, and time to symptom onset (acute vs. chronic)

are required to explain the discrepancy between clinical and radiological findings.²⁵

This challenges the previously defined cutoffs of radiological CEC and reiterates the need for future multimodal models capable of analyzing both structured clinical variables and radiological MRI scans to holistically predict the presence of true CES with CEC.

Nevertheless, in current clinical practice in most institutions, when seeing 2 patients with the exact same clinical features, surgeons are generally able to decide who needs urgent surgery, based on the amount of CEC on the MRI scan. Hence, studies like these are very relevant despite the controversy of whether the degree of CEC alone can predict who has CES or not. This study shows that models can be developed which can pick out scans with a certain degree of canal compromise.

Despite these results however, our study has a few limitations. First, the size of the dataset used for the training and testing of the model was relatively small. This may limit the ability of the model to generalize to larger and more heterogeneous patient populations. For example, cases of patients with prior hardware were excluded because of metal artifact blocking out thecal sac. Such cases would need to be included in further iterations of the model to account for real-world heterogeneity. Second, the model was developed on a single institution's dataset using mid-sagittal T2 magnetic resonance images, which may limit the ability to extrapolate the results to other institutions or different imaging protocols. In the United Kingdom, the GIRFT guidance recommends that a sagittal magnetic resonance sequence is all that is required to screen for and detect CEC. Nevertheless, analysis of the axial sequences is done by all radiologists and surgeons and the value of this in decision-making would need to be analyzed in the future fine-tuning of the model. Third, while Grad-CAM visualizations can identify potential regions containing distinctive information from MRI images, it may not entirely appreciate and discriminate between subtle details across individual patients. Finally, there exists a gray zone of overlap between the 2 outcomes groups and thus differentiating and identifying these cases may not be done reliably by our model. This suggests that further

prospective training and enhancement is required before this tool can be used in clinical practice.

CONCLUSIONS

In conclusion, this is the first study to evaluate the use of and develop computer vision ML algorithms for the automated detection and identification of CEC on MRI scans. We demonstrate that such models can be accurate and reliable in their predictions and can act as triage tools for CES referrals and facilitate neuroradiologist decision-making. Additionally, through our explainability techniques, we have demonstrated how the models' predictions can be transparent and verifiable when implemented in clinical practice. These promising results demonstrate that this technology can improve healthcare quality and care provision, with the timely diagnosis of CEC and management of CES. As referrals rise, this tool can potentially mitigate patient harm and legal risks.

CRedit AUTHORSHIP CONTRIBUTION STATEMENT

Sayan Biswas: Writing – review & editing, Writing – original draft, Investigation, Formal analysis, Data curation. **Ved Sarkar:** Writing – original draft, Software, Methodology, Conceptualization. **Joshua Ian MacArthur:** Writing – review & editing, Writing – original draft, Methodology. **Li Guo:** Writing – review & editing, Software, Methodology, Formal analysis. **Xutao Deng:** Writing – review & editing, Software, Formal analysis. **Ella Snowden:** Writing – original draft, Data curation. **Hamza Ahmed:** Writing – review & editing, Investigation, Data curation. **Callum Tetlow:** Writing – review & editing, Methodology, Investigation, Data curation. **K. Joshi George:** Writing – review & editing, Supervision, Investigation, Conceptualization.

ACKNOWLEDGMENTS

The authors wish to thank the Department of Neurosurgery at Salford Royal Hospital for providing the data.

REFERENCES

- Woodfield J, Hoeritzauer I, Jamjoom AAB, et al. Understanding cauda equina syndrome: protocol for a UK multicentre prospective observational cohort study. *BMJ Open*. 2018;8:e025230.
- Woodfield J, Hoeritzauer I, Jamjoom AAB, et al. Presentation, management, and outcomes of cauda equina syndrome up to one year after surgery, using clinician and participant reporting: a multi-centre prospective cohort study. *Lancet Reg Health Europe*. 2023;24:100545.
- Fraser S, Roberts L, Murphy E. Cauda equina syndrome: a literature review of its definition and clinical presentation. *Arch Phys Med Rehabil*. 2009; 90:1964-1968.
- Fountain DM, Davies SCL, Woodfield J, et al. Evaluation of nationwide referral pathways, investigation and treatment of suspected cauda equina syndrome in the United Kingdom. *Br J Neurosurg*. 2019;33:624-634.
- Lourenco J, Clark O. *Clinical radiology census report 2021*. United Kingdom: The Royal College of Radiologists; 2021:3-26.
- Machin JT, Hardman J, Harrison W, Briggs TWR, Hutton M. Can spinal surgery in England be saved from litigation: a review of 978 clinical negligence claims against the NHS. *Eur Spine J*. 2018;27: 2693-2699.
- Hutton M. *Spinal Services*. United Kingdom: GIRFT Programme National Specialty Report; 2009: 5-100.
- Gardner A, Gardner E, Morley T. Cauda equina syndrome: a review of the current clinical and medico-legal position. *Eur Spine J*. 2011;20: 690-697.
- Investigation report: Timely detection and treatment of cauda equina syndrome. Healthcare Safety Investigation Branch; 2022. Available at: <https://www.hssib.org.uk/patient-safety-investigations/timely-detection-and-treatment-of-spinal-nerve-compression-cauda-equina-syndrome-in-patients-with-back-pain/investigation-report/>. Accessed February 12, 2025.
- Altun S, Alkan A. LSS-net: 3-dimensional segmentation of the spinal canal for the diagnosis of lumbar spinal stenosis. *Int J Imaging Syst Tech*. 2023;33:378-388.

11. Altun S, Alkan A. Lumbar spinal stenosis analysis with deep learning based decision support systems. *Gazi University J Sci.* 2023;36:1200-1215.
12. Fairbank J, Hashimoto R, Dailey A, Patel AA, Dettori JR. Does patient history and physical examination predict MRI proven cauda equina syndrome? *Evid Based Spine Care J.* 2011;2:27-33.
13. Simonyan K, Zisserman A. Very deep convolutional networks for large-scale image recognition. *arXiv.org*; 2025. Available at: <https://arxiv.org/abs/1409.1556>. Accessed February 12, 2025.
14. He K, Zhang X, Ren S, Sun J. Deep residual learning for image recognition. 2016 *IEEE Conference on Computer Vision and Pattern Recognition (CVPR)*; 2016:770-778. Available at: <https://doi.org/10.1109/cvpr.2016.90>. Accessed February 12, 2025.
15. Huang G, Liu Z, Van Der Maaten L, Weinberger KQ. Densely connected convolutional networks. 2017 *IEEE Conference on Computer Vision and Pattern Recognition (CVPR)*; 2017:2261-2269. Available at: <https://doi.org/10.1109/cvpr.2017.243>. Accessed February 12, 2025.
16. Dosovitskiy A, Beyer L, Kolesnikov A, et al. An Image is Worth 16x16 Words: Transformers for Image Recognition at Scale. *arXiv:2010.11929 [cs]*; 2020. Available at: <https://arxiv.org/abs/2010.11929>. Accessed February 12, 2025.
17. Deng J, Dong W, Socher R, Li LJ, Li K, Fei-Fei L. ImageNet: A large-scale hierarchical image database. 2009 *IEEE Conference on Computer Vision and Pattern Recognition*; 2009. Available at: <https://doi.org/10.1109/cvpr.2009.5206848>. Accessed February 12, 2025.
18. Sudirman S, Al Kafri A, Natalia F, et al. Lumbar spine MRI dataset. *datamendeleycom*; 2019. <https://doi.org/10.17632/k57fr854j2.2>. Accessed February 12, 2025.
19. He K, Chen X, Xie S, Li Y, Dollár P, Girshick R. Masked autoencoders are scalable vision learners. *ICLR 2021 Conference*; 2021.
20. Selvaraju RR, Cogswell M, Das A, Vedantam R, Parikh D, Batra D. Grad-CAM: visual explanations from deep networks via gradient-based localization. *Int J Comput Vis.* 2020;128:336-359.
21. Hogan WB, Kuris EO, Durand WM, Eltorai AEM, Daniels AH. Timing of surgical decompression for cauda equina syndrome. *World Neurosurg.* 2019;132:e732-e738.
22. Bell DA, Collie D, Statham PF. Cauda equina syndrome – what is the correlation between clinical assessment and MRI scanning? *British. J Neurosurg.* 2007;21:201-203.
23. Balasubramanian K, Kalsi P, Greenough CG, Kuskoor Seetharam MP. Reliability of clinical assessment in diagnosing cauda equina syndrome. *Br J Neurosurg.* 2010;24:383-386.
24. McCarthy M, Brodie A, Aylott C, Annesley-Williams D, Jones A, Grevitt M. MRI measurements in Cauda Equina Syndrome: reproducibility and prediction of clinical outcome. *Orthop Proc.* 2006;88-B:147-148.
25. Kaiser R, Nasto LA, Venkatesan M, et al. Time factor and disc herniation size: are they really predictive for outcome of urinary dysfunction in patients with cauda equina syndrome? *Neurosurgery.* 2018;83:1193-1200.

Conflict of interest statement: The authors declare that the article content was composed in the absence of any commercial or financial relationships that could be construed as a potential conflict of interest.

Previous presentation: Oral presentation at the Society of British Neurological Surgeons (SBNS) 2024 Conference, Edinburgh.

Received 21 November 2024; accepted 8 January 2025

Citation: World Neurosurg. (2025) 195:123669. <https://doi.org/10.1016/j.wneu.2025.123669>

Journal homepage: www.journals.elsevier.com/world-neurosurgery

Available online: www.sciencedirect.com

1878-8750/© 2025 The Authors. Published by Elsevier Inc. This is an open access article under the CC BY license (<http://creativecommons.org/licenses/by/4.0/>).